IEEE Access
Multidisciplinary | Rapid Review | Open Access Journal

Received 9 May 2023, accepted 9 June 2023, date of publication 13 June 2023, date of current version 28 June 2023.

Digital Object Identifier 10.1109/ACCESS.2023.3285619

RESEARCH ARTICLE

Wideband Wide Beam-Width Modified Angled Dipole Antenna for 5G Millimeter-Wave IoT Applications

TAE HWAN JANG[1], (Member, IEEE), AHNWOO LEE[1], SUNGHYUK KIM[1], HEE SUNG LEE[2], JAESUK LEE[3], HOON-GEUN SONG[3], AND JUNG HYUN KIM[1], (Senior Member, IEEE)

[1]School of Electronic Engineering, Hanyang University ERICA, Ansan 15588, Republic of Korea
[2]Samsung Research, Samsung Electronics, Seoul 06765, South Korea
[3]Korea Testing Laboratory, Ansan 15588, South Korea

Corresponding authors: Sunghyuk Kim (kimsh96@hanyang.ac.kr) and Jung Hyun Kim (junhkim@hanyang.ac.kr)

This work was supported by the Institute of Information and Communications Technology Planning and Evaluation (IITP) Grant funded by the Korea Government (MSIT) (High-Resolution Vector Network Analyzer SW Development Supporting Sub-THz Frequency Band) under Grant 2022-0-00859.

ABSTRACT In this work, a millimeter-wave wideband wide beamwidth modified angled dipole antenna is proposed for 5G millimeter-wave(mmW) IoT applications. The modified angled dipole antenna which has a dipole arm that is bent once more perpendicular to the ground plane compared to the existing angled dipole is proposed to improve not only the beamwidth but also the S_{11} bandwidth. The image current is formed in the direction perpendicular to the ground by the dipole arm bent to be orthogonal to the ground. Because only the E-field in the direction perpendicular to the ground can be formed by the boundary condition, the E-field radiated from the proposed antenna can be radiated along the ground plane, and thus the E-plane beamwidth is widened, and the H–plane beamwidth can be widened. The measured -10 dB S_{11} bandwidth is 5 GHz(=17.8%) ranging from 25.7 GHz to 30.7 GHz, and the measured HPBW is 160° ±5 ° and 310°±10° for the E-plane and H-plane, respectively. To verify whether the proposed antenna is practically applied to 5G IoT applications, the beamforming IC was connected to the proposed antenna array, and the E-plane beam-forming radiation pattern was measured. Although it was applied only to the $-90° \leq \beta \leq 90°$ range, the -3 dB E-plane beamwidth was 130°, ensuring wide coverage.

INDEX TERMS Dipole antenna, angled dipole, beamwidth, bandwidth, millimeter-wave (mmW).

I. INTRODUCTION

Compare to that conventional communication networks, the next generation (5G) network is expected to provide significantly improved performance such as increased capacity thanks to the millimeter-wave (mm-Wave) 5G spectrum [1], [2]. Moreover, the combination of the fifth-generation (5G) communication and the Internet of Things (IoT) have started to wirelessly connect people, data, processes, and infrastructure with high data rates and low latency [3]. Cisco Systems recently reported that 29.3 billion networked IoT devices will operate by 2023, outnumbering humans by more than threefold [4]. These applications are expected to be crucial in the development of the IoT industry as they support wireless high-speed connections between devices.

However, different from the designing antennas for 4G applications, increasing the operating frequency would bring several issues and challenges in the antenna design concepts for the 5G mobile devices which need new techniques [5], [6], [7], [8], [9], [10], [11].

In order to utilize the mmW frequency, a beam-forming technique should be used to cover the severe path loss. In general, since the beamwidth of an antenna is limited by the beamwidth of an individual antenna, it is essential to design an antenna element having a wide

The associate editor coordinating the review of this manuscript and approving it for publication was Hussein Attia.

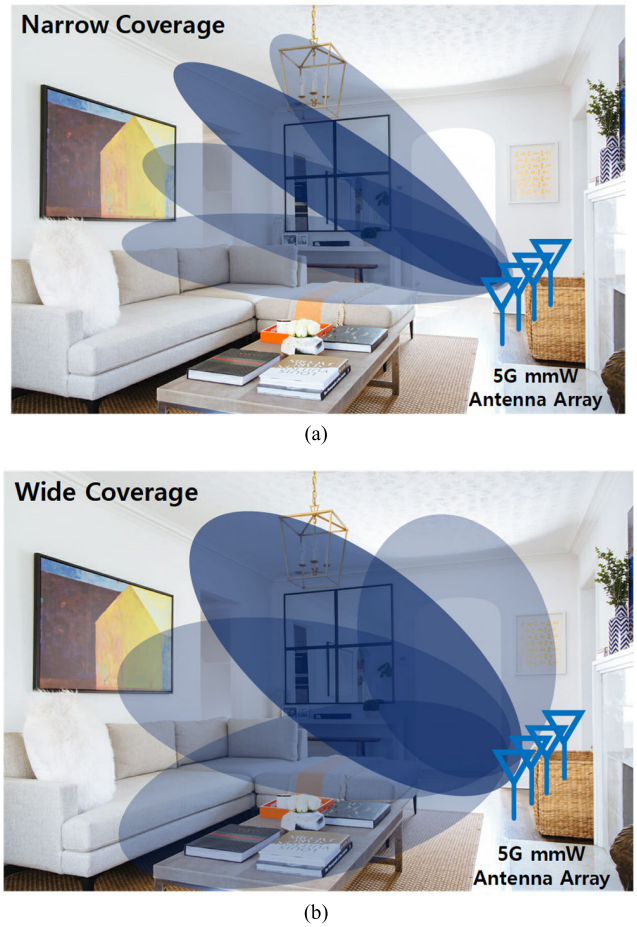

FIGURE 1. Two possible scenarios in 5G mmW IoT applications. (a) narrow coverage and (b) wide coverage.

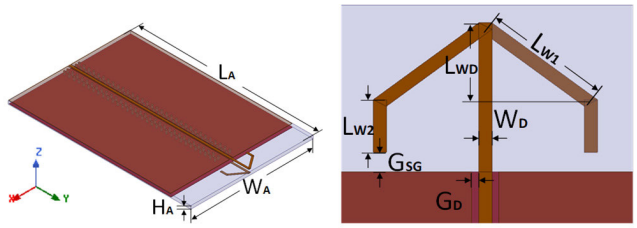

FIGURE 2. Geometry of proposed antenna. (a) 3-D view and (b) top view The parameter dimensions in millimeters are $L_A = 22.5$, $W_A = 15$, $H_A = 0.38$, $L_{W1} = 1.98$, $L_{W2} = 0.8$, $G_{SG} = 0.3$, $W_D = 0.2$, $L_{WD} = 1.2$ and $G_D = 0.105$.

beamwidth so as to cover all randomly located mobile terminals.

Among the wireless technologies in the mmW band, antenna-in-package (AiP) technology [12], [13], [14], [15], [16], [17] that enables communication in various mobile environments is important. AiPs for millimeter-wave (mmW) mobile devices generally consider a structure consisting of antennas revealing broadside radiation and end-fire radiation [17]. In case of handheld mobile device, such as a

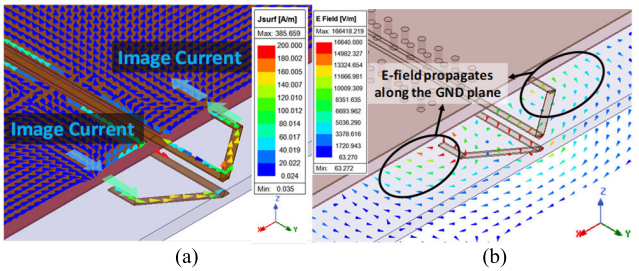

FIGURE 3. The (a) current distribution and (b) E-field distribution of the proposed antenna.

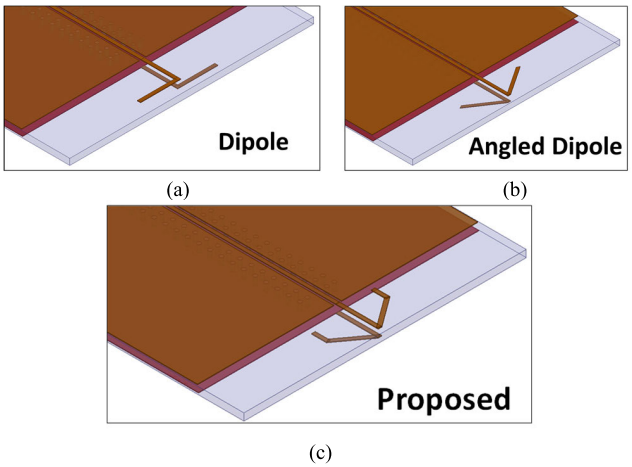

FIGURE 4. Geometry of the (a) original dipole antenna, (b) angled dipole antenna and (c) proposed modified angled dipole antenna.

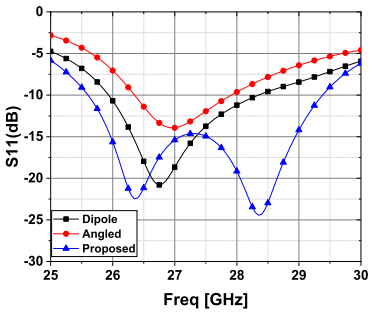

FIGURE 5. S_{11} of the dipole antenna, angled dipole antenna and proposed modified angled dipole antenna.

smartphone, the radiation conditions of the device could be changed depending on the user's posture and environment. Therefore, wider coverage of AiPs are preferable. Fig. 1 indicates two possible scenarios in 5G millimeter-wave IoT applications. Compared to an antenna with a narrow beamwidth, an antenna with a wide beamwidth has a much wider coverage, so it can communicate with much more IoT devices. In that point, AiPs must be located on all sides of the device to have wide coverage. Generally, broadside antennas in AiPs typically consist of a micro-strip patch antenna structure [18], [19], [20], [21] located on the top layer of the substrate such as E-shaped structure [18], [19], [20], [21],

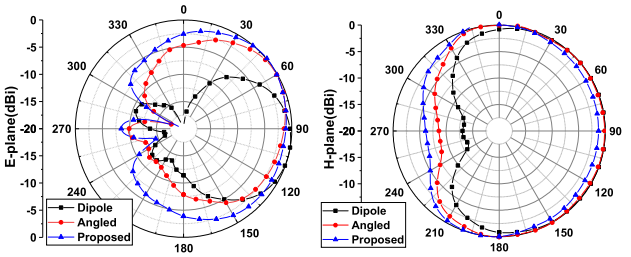

FIGURE 6. Normalized (a) E-plane and (b) H-plane radiation pattern of the dipole antenna, angled antenna and proposed modified angled dipole antenna.

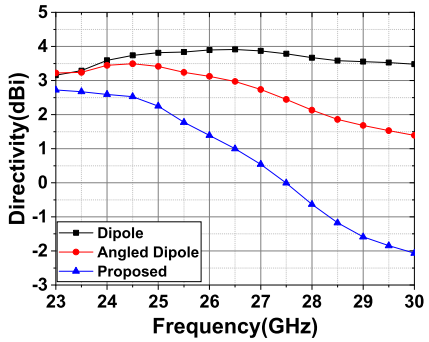

FIGURE 7. Simulated end-fire directivity of the dipole antenna, angled antenna and proposed modified angled dipole antenna.

U-slot structure [22], [23], [24], [25], L-probe structure [26], [27], [28] and parasitic patch [24], [29], [30]. That's because the micro-strip patch antenna is a typical planar antenna that radiate broadside wave and this type is most commonly used thanks to its simple structure and low manufacturing cost and moderate radiation performance. The end-fire antennas for the AiP are typically consist of dipole antenna [31], [32], [33] thanks to the planar structure. This type of antenna commonly has a ground shield reflector, which is the back-side of the radiator, to focus the beam to the front of the antenna. However, this conventional structure is basically suffer from limited beamwidth around ±45°, and this leads to the limited scanning range due to the limited antenna element. In [34], [35], [36], [37], [38], and [39], to improve the beamwidth performance of the dipole antenna, angled type dipole antenna is proposed. The E-plane beamwidth is broaden to ±65°. However, in order to further expand the coverage for practical use in actual beam-forming, an antenna having a wider beam-width of the E- and H-plane is essential.

In this work, modified angled dipole antenna which has dipole arm which is bent once more perpendicular to the ground plane compared to the existing angled dipole is proposed to improve not only the beamwidth but also S_{11} bandwidth. The proposed antenna is designed to cover the 28 GHz 5G n257 band (26.5 GHz - 29.5 GHz). Section II describes the design procedure of the proposed antenna, and Section III presents the measurements of the antenna.

TABLE 1. Comparison table of the proposed dipole antenna with a reference structure.

Type	S_{11} BW (%, GHz-GHz)	3-dB E-Plane Beamwidth (°)	3-dB H-Plane Beamwidth (°)
Dipole	8.7%, 25.9-28.3	76° (64° ~140°)	228° (-24° ~ 204°)
Angled	5.9%, 26.3-27.9	126° (16° ~142°)	258° (-36° ~ 222°)
Proposed	13%, 25.6-29.4	176° (-4° ~ 172°)	286° (-56° ~ 230°)

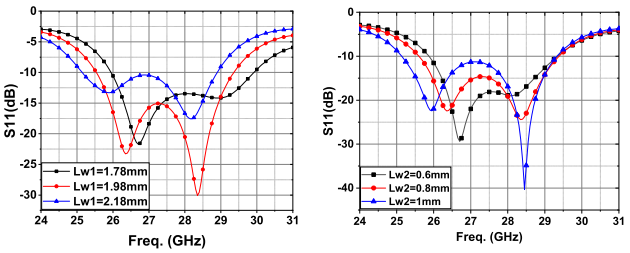

FIGURE 8. Simulated S_{11} of the proposed antenna by sweeping (a) L_{W1} and (b) L_{W2}.

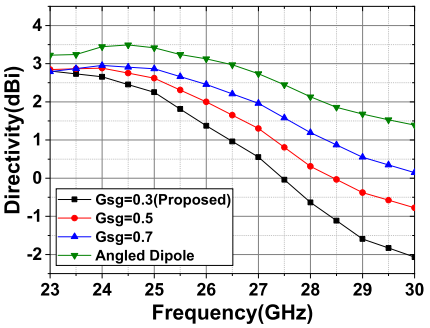

FIGURE 9. Simulated directivity the proposed antenna by sweeping G_{SG}.

II. ANTENNA DESIGN

In this work, wideband wide beamwidth dipole antenna is presented to cover the 5G n257 millimeter wave frequency band for actual use. Fig. 3 shows the geometry of proposed antenna. In this study, a Taconic TLY-5 substrate with a thickness of 0.38 mm, a dielectric permittivity (ε_r) of 2.2, and a metal thickness (t) of 18um was chosen. As the antenna will be measured through a ground-signal-ground (G-S-G) probe, the antenna is fed through the ground-backed coplanar waveguide (GCPW). The antenna was designed using the 3-D full-wave electromagnetic solver. Compared to the angled dipole antenna, the proposed antenna is designed to bend the dipole arm once more to be perpendicular to the ground plane. By doing so, it is possible to secure the advantage of widening the E- and H-plane beamwidths and S_{11} bandwidth compared to the existing dipole antenna and the angled dipole antenna.

The proposed antenna will be measured using the GCPW to coaxial transition, and the L_A length of the antenna was secured to 20mm or more so that the radiation pattern is not affected as much as possible by the transition made of metal.

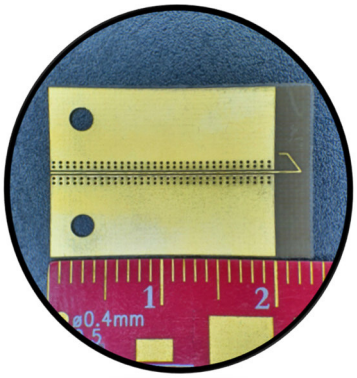

FIGURE 10. Fabricated antenna.

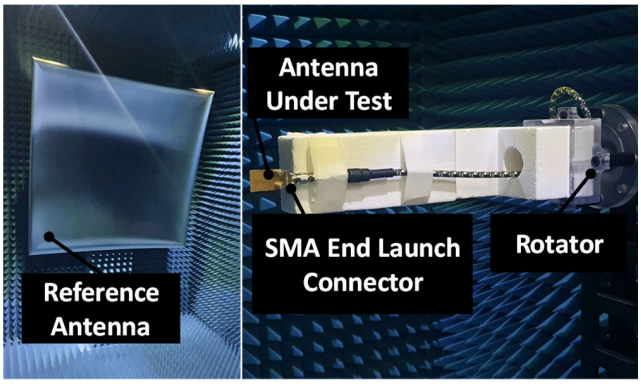

(a) (b)

FIGURE 11. The antenna radiation pattern measurement setup. (a) front side, (b) back side.

Through holes connecting top metal plate and bottom metal plate are placed in the ground plate around the signal line so that the signal wave does not flow between the top metal and the ground metal. The length of the dipole(=$2(L_{W1} + L_{W2})$) is set to 5.5 mm (= $0.65\lambda_{eff}$), and space between ground plane and dipole arm (= $L_{WD} + L_{W2} + G_{SG}$) is set to 2.3mm(= $0.23\lambda_0$) to optimize the radiation pattern, where λ_0 is the free space wavelength at the 28 GHz frequency. Fig. 2 shows the current distribution and the E-field distribution of the proposed antenna. In the case of a conventional dipole antenna, since the current distribution is formed to be parallel to the ground, an E-field parallel to the ground cannot be formed. Therefore, E-plane and H-plane radiation patterns are limited by the ground plane because radio waves cannot radiate in the direction of the ground plane.

In the case of an angled dipole, it is possible to not only radiate in the end-fire direction by bending the dipole arm at an acute angle, but also in the diagonal direction. Therefore, it is possible to secure a wider beam width than the existing dipole antenna. Nevertheless, since there is a parallel current to the ground, the E-field does not exist near the ground, so the beam widths of the E-plane and H-plane are also limited by the ground plane. Therefore, for a wide beamwidth, additional structures need to be studied so as not to be constrained by the ground plane. However, in case of the proposed antenna, image current is formed in the direction perpendicular to the ground by the dipole arm bent to be orthogonal to the ground. Because only the E-field in the direction perpendicular to the ground can be formed by the boundary condition, the E-field radiated from the proposed antenna can be radiated along the ground plane, and thus the E-plane beamwidth is widened, and the H -plane beamwidth can be widened. In addition, the image current formed in the ground and the dipole arm erected perpendicular to the ground form an additional resonant frequency, so that the bandwidth of S_{11} is also be widen. In fact, it can be seen that the image current flows perpendicular to the ground in the same direction as the current flowing through the dipole arm. In addition, it can be confirmed that the E-field radiated from the proposed antenna is radiated along the ground.

Fig. 4 shows the geometry of the original dipole antenna, angled dipole antenna and the proposed modified angled dipole antenna. In order to compare the performance of the actual proposed antenna with that of the existing antenna, the reference structure of the existing antenna was designed, and the S_{11} performance and the radiation pattern performance were compared. Fig. 5 shows the S_{11} of the dipole antenna, angled dipole antenna and proposed modified angled dipole antenna. The original dipole antenna shows 8.7% S_{11} bandwidth covering 25.9 to 28.3 GHz frequency and the angled dipole antenna shows 5.9% S_{11} bandwidth ranging from 26.3 GHz to 27.9 GHz frequency. The angled dipole and original dipole have only one resonance frequency generated by the dipole arm, showing narrowband characteristics. In addition, in the case of the angled dipole, the beamwidth increases, but the S_{11} bandwidth is narrower than that of the original dipole because the radiated wave cannot propagate to the outside and is stored due to the angle of the antenna is narrow. But the proposed modified angled dipole antenna shows 13% fractional bandwidth covering 25.6 GHz to 29.4 GHz frequency band. The proposed antenna shows wide bandwidth compared to that of the reference structure because it reveals two resonance frequencies.

Fig. 6 shows the normalized E-plane radiation pattern of the dipole antenna, angled antenna, and proposed modified angled dipole antenna. The E-plane beamwidth is 76°, 126° and 176°, respectively for original dipole, angled dipole and the proposed antenna. The H-plane beamwidth is 228°, 258° and 286°, respectively for original dipole, angled dipole and the proposed antenna. As mentioned above, since the E-field radiated from the dipole arm arranged perpendicular to the ground of the proposed antenna is radiated along the ground, an E-plane beamwidth close to 180° can be obtained. Since the H-plane also covers 286°, it can be seen that the proposed antenna covers at least the hemisphere.

Fig. 7 shows the simulated end-fire directivity of the dipole antenna, angled antenna and proposed modified angled dipole antenna. In the case of the angled dipole, the directivity in the end-fire direction is lower than in the case of the dipole, and in the case of the proposed dipole, the directivity is

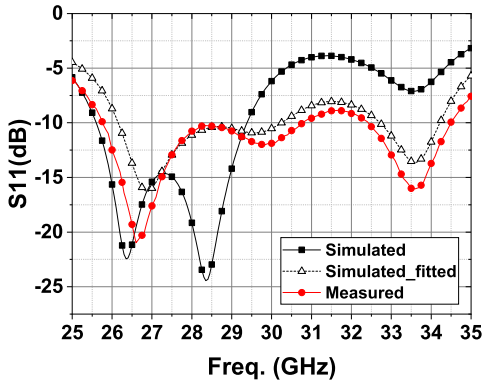

FIGURE 12. Simulated and measured S_{11} of the proposed antenna.

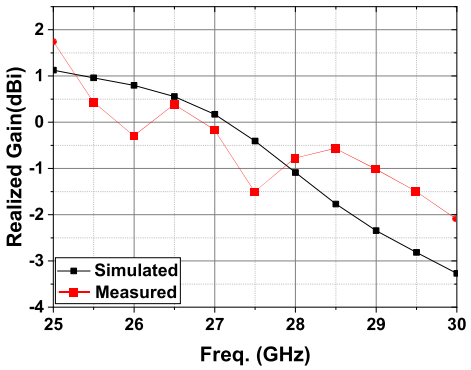

FIGURE 13. Simulated and measured end-fire gain of the proposed antenna.

lower than in the case of the angled dipole. The reduction in directivity is more prominent in the higher resonance region of the proposed dipole(=28.4 GHz), and in this frequency band, the field due to vertical resonance is radiated along the ground and the radiation width becomes wider, so it can be confirmed that the directivity comes out lower.

Fig. 8 shows the simulated S_{11} of the proposed antenna by sweeping $\mathbf{L_{W1}}$ and $\mathbf{L_{W2}}$. By controlling the $\mathbf{L_{W1}}$, the overall resonance frequencies are controlled, and the lower resonance frequency is controlled by controlling the $\mathbf{L_{W2}}$. If $\mathbf{L_{W2}}$ is adjusted, the length of the image current in the ground is also adjusted, so it can be seen that the low resonance frequency is controlled by the length of the image current. By adjusting $\mathbf{L_{W1}}$, not only the length of the original dipole arm but also the length of the image current increases, so overall resonant frequencies are controlled by $\mathbf{L_{W1}}$. The optimized $\mathbf{L_{W1}}$ and $\mathbf{L_{W2}}$ values were selected to maximize the bandwidth of the proposed antenna. Table 1 shows the comparison table of the proposed dipole antenna with reference structure. It is clearly shown that the proposed modified angled structure reveals not only wide S_{11} bandwidth but also wide E- and H-plane beamwidth compared to the reference structure. Since the proposed antenna shows a wide beamwidth that covers the hemisphere, it can be widely used to obtain wide coverage in the 5G n257 millimeter wave frequency band.

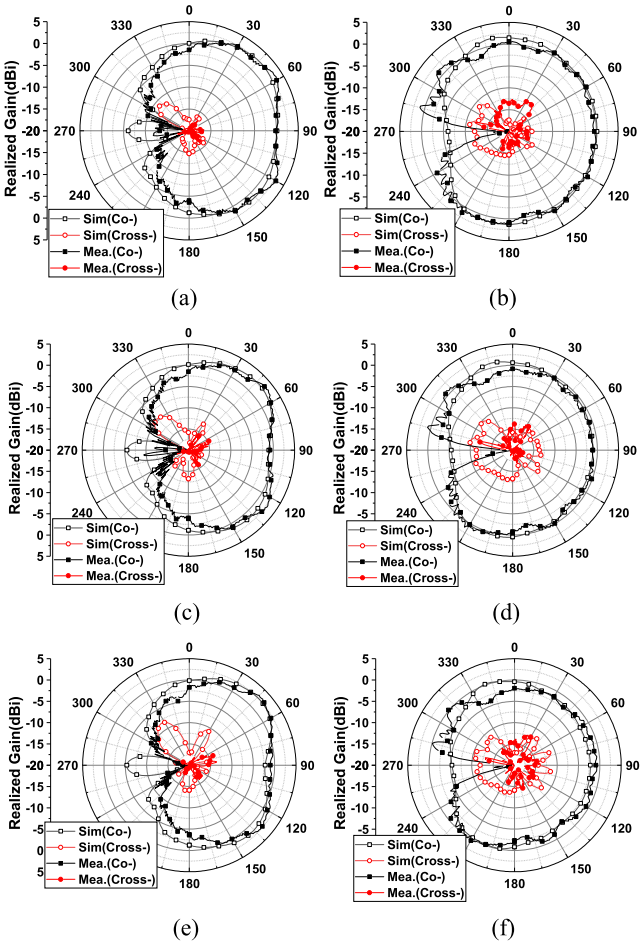

FIGURE 14. Simulated and measured radiation pattern of the proposed antenna. (a) 27-GHz E-plane, (b) 27-GHz H-plane, (c) 28-GHz E-plane (d) 28 GHz H-plane, (e) 29-GHz E-plane and (f) 29-GHz H-plane.

TABLE 2. Simulated and measured performance of the proposed dipole antenna.

Parameter	Simulated	Measured
Real. Gain (dBi)	-1 dBi	0.7 dBi
S_{11} BW(%) (GHz-GHz)	14.6 % (25.6-29.4)	30.0 %* (25.7-34.7)
E-plane HPBW (°)	176°	160° ± 5 °
H-plane HPBW (°)	286°	310° ± 10°

* -9dB S_{11} BW.

Fig. 9 shows the simulated directivity the proposed antenna by sweeping G_{SG}. As G_{SG} increases, the directivity of the antenna increases, which corresponds to a decrease in beam width. This is actually because the farther the distance between the arm of the antenna and the ground, the less effective the radiated field travels to the ground.

III. ANTENNA MEASUREMENT

Fig. 10 shows the fabricated antenna. The proposed antenna was measured within 25 GHz – 30 GHz frequency band,

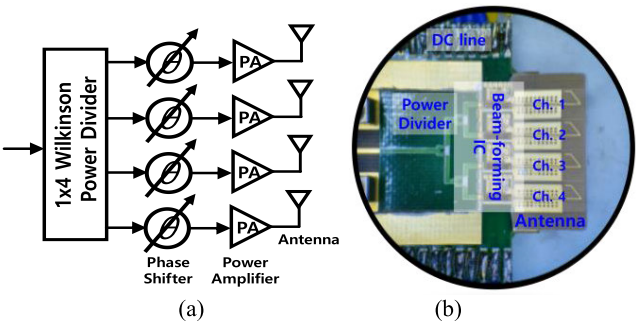

FIGURE 15. The (a) schematic and (b) micrograph of the fabricated beamforming AiP module using proposed antenna.

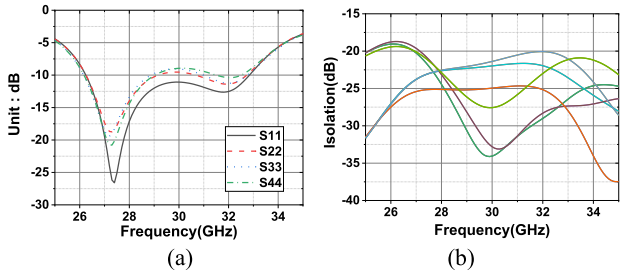

FIGURE 16. Simulated S-parameters of the proposed array antenna. (a) S_{11} performance and (b) Isolation.

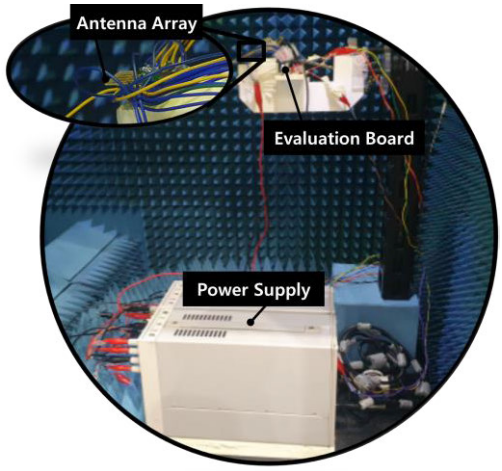

FIGURE 17. The antenna radiation pattern measurement setup for beamforming AiP.

and the return loss was measured by a probing GSG probe connected to a vector network analyzer (VNA). Fig. 11 shows the antenna radiation pattern measurement setup. The antenna is measured in the anechoic chamber. The radiation of the fabricated antenna was measured using the coaxial connector for feeding, and the AUT(antenna under test) performance (realized gain, radiation pattern, cross-polarization, etc.) was calculated and derived by measuring the proximity electric field in the near-field region of the AUT. Fig. 12 shows the simulated and measured S_{11} of the proposed antenna. The simulated -10 dB S_{11} bandwidth is 3.8 GHz(=14.2%) ranging from 25.6 GHz to 29.4 GHz, and the measured -10 dB S_{11}

TABLE 3. Comparison table of the wide beamwidth dipole antenna.

	Real. Gain	S_{11} BW(%) (GHz-GHz)	E-plane HPBW (°)	H-plane HPBW (°)
[34]	2.5 dBi	26.9 % (20.0–26.2)	110°	240°
[35]	5.8 dBi	36.2 % (26.5–38.2)	66°	152°
[36]	5.3 dBi	81.1 % (3.3-7.8)	111°	103°
[37]	6.2 dBi	24.9 % (0.4-0.51)	87°	N/A
This work	-0.7 dBi @ 28 GHz	30.0 %* (25.7-34.7)	160° ± 5 °	310° ± 10°

* -9 dB S_{11} BW.

bandwidth is 5 GHz(=17.8%) ranging from 25.7 GHz to 30.7 GHz. When comparing the simulation and measurement results, the measured high resonant frequency is down shifted as much as 1.2 GHz from the simulated resonant frequency corresponds to 29.6 GHz. This is presumed to be the result of G_{SG} value being produced differently from the simulation($G_{SG} = 0.45$mm).

Fig. 13 shows the simulated and measured end-fire gain of the proposed antenna. Since the proposed antenna maximizes the beamwidth, the gain in the end-fire direction is around 0 dBi. The deviation between the simulated and measured gain is within 1.3 dB. Fig. 14 shows the simulated and measured radiation pattern of the proposed antenna. The radiation pattern is measured at 27 GHz, 28 GHz and 29 GHz, respectively. The measured HPBW is $160° \pm 5°$ and $310° \pm 10°$ for the E-plane and H-plane, respectively. The difference between measured and simulated gain is as low as 1.1 dB, and it is presumed to be the result of radio waves radiated from the antenna being reflected from surrounding structures (adapter, coaxial cable …). The cross-polarization level is at least lower than -13 dBi. From the results, the proposed antenna successfully covers 5G n257 band while revealing wide beamwidth. Based on the simulated and measured data, the Table 2 summarize the simulated and measured performance of the proposed dipole antenna.

Fig. 15 shows the micrograph of the fabricated antenna in a package(AiP) module. The IC is fabricated in 0.15-μm GaAs pHEMT process. Each beamforming IC was arranged for each channel and connected through an off-chip power divider. The presented antenna in package is fabricated for transmitting operation.

The power is divided into 4 parts by the Wilkinson power splitter, the phase of the channel is adjusted by the phase shifter in each channel, and finally amplified by the power amplifier and connected to the antenna. The power divider was manufactured using a Taconic TLY-5 board. The area of the overall beamforming IC is $3700 \times 950 \mu m^2$. In order to verify the actual beamforming characteristics, a 1×4 dipole antenna was manufactured and packaged with a beamforming IC. For the AiP, the bias lines are connected to the chip through bond-wires to operate the beamforming IC.

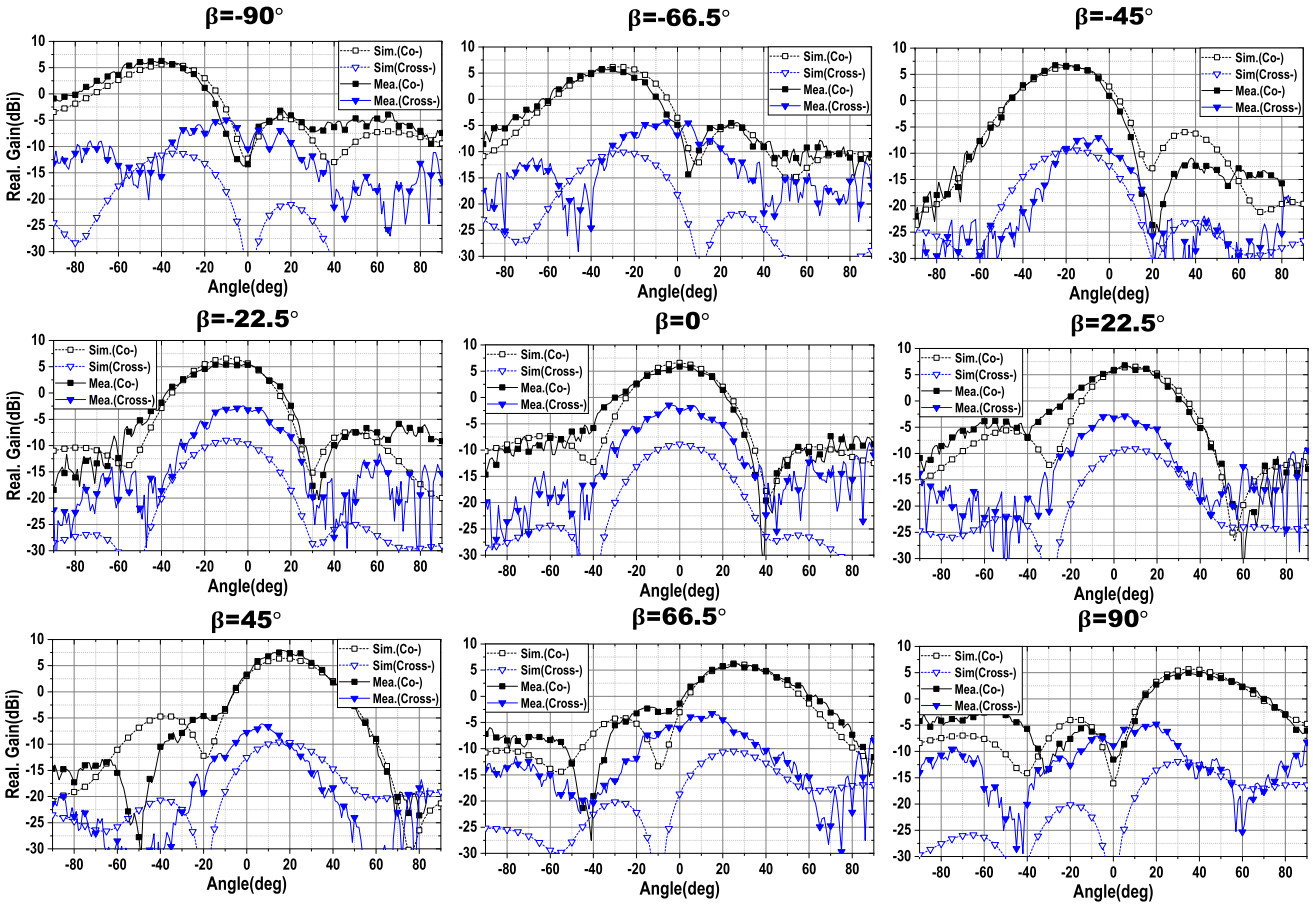

FIGURE 18. The simulated and measured E-plane beam-forming radiation pattern for the proposed antenna in package at 28 GHz.

The radiation pattern is measured in -90 ° $\leq \beta \leq$ 90 ° range because the sidelobe is high in other areas.

Fig. 16. shows the simulated S-parameters of the proposed array antenna. Although interference between antennas occurs, isolation is managed to less than -18 dB within a given band, and S_{11} is managed to less than -8.9 dB at most, which causes a maximum reduction of only 0.58 dB in efficiency by impedance matching.

Fig. 17 shows the antenna radiation pattern measurement setup for beamforming AiP. The antenna array was also measured in an anechoic chamber.

Fig. 18 shows the simulated and measured E-plane beamforming radiation pattern for the proposed antenna in package at 28 GHz. Although the usable range is set to -90 ° $\leq \beta \leq$ 90°, the 3-dB coverable range of the proposed AiP is 130 ° ranging from -66 ° to 64 °. It was confirmed that the beam-forming characteristics agree well with the simulation for the usable range of -90 ° $\leq \beta \leq$ 90 °. From the simulated and measured radiation pattern, it can be seen that cross-polarization and sidelobe level are higher than the simulation because this is presumed to be an effect caused by the reflection or refracting of the wave radiated from the antenna by the surrounding evaluation board or the other electrical components. This also may caused by the misalignment of the measurement setup or the dimensions of the fabricated antenna being slightly different from that of the simulated one. Table 3 shows the comparison table of the wide beamwidth dipole antenna. The proposed antenna shows the widest E-plane and H-plane beamwidth among the reported dipole antenna.

IV. CONCLUSION

Millimeter-wave wideband wide beamwidth modified angled dipole antenna is proposed for 5G mmW IoT applications. The modified angled dipole antenna which has a dipole arm which is bent once more perpendicular to the ground plane compared to the existing angled dipole is proposed to improve beamwidth as well as the bandwidth. The measured -10 dB S_{11} bandwidth is 5 GHz(=17.8%) ranging from 25.7 GHz to 30.7 GHz, and the measured HPBW is 150° ±5 ° and 310°±10° for the E-plane and H-plane, respectively. To verify whether the proposed antenna is practically applied to 5G IoT applications, the beamforming IC was connected to the proposed antenna array, and the beamforming radiation pattern was verified.

ACKNOWLEDGMENT

The EDA tool was supported by the IC Design Education Center (IDEC), South Korea.

REFERENCES

[1] A. Osseiran, F. Boccardi, V. Braun, K. Kusume, P. Marsch, M. Maternia, O. Queseth, M. Schellmann, H. Schotten, H. Taoka, H. Tullberg, M. A. Uusitalo, B. Timus, and M. Fallgren, "Scenarios for 5G mobile and wireless communications: The vision of the METIS project," *IEEE Commun. Mag.*, vol. 52, no. 5, pp. 26–35, May 2014.

[2] W. Roh, J. Seol, J. Park, B. Lee, J. Lee, Y. Kim, J. Cho, K. Cheun, and F. Aryanfar, "Millimeter-wave beamforming as an enabling technology for 5G cellular communications: Theoretical feasibility and prototype results," *IEEE Commun. Mag.*, vol. 52, no. 2, pp. 106–113, Feb. 2014.

[3] L. Chettri and R. Bera, "A comprehensive survey on Internet of Things (IoT) toward 5G wireless systems," *IEEE Internet Things J.*, vol. 7, no. 1, pp. 16–32, Jan. 2020.

[4] [Online]. Available: https://www.cisco.com/c/en/us/solutions/collateral/executiveperspectives/annual-internet-report/white-paper-c11-741490.html

[5] W. Hong, K. Baek, and S. Ko, "Millimeter-wave 5G antennas for smartphones: Overview and experimental demonstration," *IEEE Trans. Antennas Propag.*, vol. 65, no. 12, pp. 6250–6261, Dec. 2017.

[6] S. Zhang, I. Syrytsin, and G. F. Pedersen, "Compact beam-steerable antenna array with two passive parasitic elements for 5G mobile terminals at 28 GHz," *IEEE Trans. Antennas Propag.*, vol. 66, no. 10, pp. 5193–5203, Oct. 2018.

[7] M. M. S. Taheri, A. Abdipour, S. Zhang, and G. F. Pedersen, "Integrated millimeter-wave wideband end-fire 5G beam steerable array and low-frequency 4G LTE antenna in mobile terminals," *IEEE Trans. Veh. Technol.*, vol. 68, no. 4, pp. 4042–4046, Apr. 2019.

[8] W. Hong, K.-H. Baek, Y. Lee, Y. Kim, and S. Ko, "Study and prototyping of practically large-scale mmWave antenna systems for 5G cellular devices," *IEEE Commun. Mag.*, vol. 52, no. 9, pp. 63–69, Sep. 2014.

[9] S. A. Ali, M. Wajid, A. Kumar, and M. S. Alam, "Design challenges and possible solutions for 5G SIW MIMO and phased array antennas: A review," *IEEE Access*, vol. 10, pp. 88567–88594, 2022.

[10] I.-J. Hwang, J.-I. Oh, H.-W. Jo, K.-S. Kim, J.-W. Yu, and D.-J. Lee, "28 GHz and 38 GHz dual-band vertically stacked dipole antennas on flexible liquid crystal polymer substrates for millimeter-wave 5G cellular handsets," *IEEE Trans. Antennas Propag.*, vol. 70, no. 5, pp. 3223–3236, May 2022.

[11] W. Hong, Z. H. Jiang, C. Yu, D. Hou, H. Wang, C. Guo, Y. Hu, L. Kuai, Y. Yu, Z. Jiang, Z. Chen, J. Chen, Z. Yu, J. Zhai, N. Zhang, L. Tian, F. Wu, G. Yang, Z. Hao, and J. Y. Zhou, "The role of millimeter-wave technologies in 5G/6G wireless communications," *IEEE J. Microw.*, vol. 1, no. 1, pp. 101–122, Jan. 2021.

[12] H. Kim and S. Nam, "Performance enhancement of 5G millimeter wave antenna module integrated tablet device," *IEEE Trans. Antennas Propag.*, vol. 69, no. 7, pp. 3800–3810, Jul. 2021.

[13] A. Rashidian, S. Jafarlou, A. Tomkins, K. Law, M. Tazlauanu, and K. Hayashi, "Compact 60 GHz phased-array antennas with enhanced radiation properties in flip-chip BGA packages," *IEEE Trans. Antennas Propag.*, vol. 67, no. 3, pp. 1605–1619, Mar. 2019.

[14] X. Gu, D. Liu, C. Baks, O. Tageman, B. Sadhu, J. Hallin, L. Rexberg, P. Parida, Y. Kwark, and A. Valdes-Garcia, "Development, implementation, and characterization of a 64-element dual-polarized phased-array antenna module for 28-GHz high-speed data communications," *IEEE Trans. Microw. Theory Techn.*, vol. 67, no. 7, pp. 2975–2984, Jul. 2019.

[15] H. Y. Kim, T. H. Jang, H. H. Bae, and C. S. Park, "A 60 GHz compact multidirectional-beam antenna-in-package for mobile devices," *IEEE Antennas Wireless Propag. Lett.*, vol. 18, no. 11, pp. 2434–2438, Nov. 2019.

[16] Y. Zhang and J. Mao, "An overview of the development of antenna-in-package technology for highly integrated wireless devices," *Proc. IEEE*, vol. 107, no. 11, pp. 2265–2280, Nov. 2019.

[17] X. Gu, D. Liu, C. Baks, B. Sadhu, and A. Valdes-Garcia, "A multilayer organic package with four integrated 60 GHz antennas enabling broadside and end-fire radiation for portable communication devices," in *Proc. IEEE 65th Electron. Compon. Technol. Conf. (ECTC)*, May 2015, pp. 1005–1009.

[18] F. Yang, X.-X. Zhang, X. Ye, and Y. Rahmat-Samii, "Wide-band E-shaped patch antennas for wireless communications," *IEEE Trans. Antennas Propag.*, vol. 49, no. 7, pp. 1094–1100, Jul. 2001.

[19] T. H. Jang, H. Y. Kim, I. S. Song, C. J. Lee, J. H. Lee, and C. S. Park, "A wideband aperture efficient 60-GHz series-fed E-shaped patch antenna array with copolarized parasitic patches," *IEEE Trans. Antennas Propag.*, vol. 64, no. 12, pp. 5518–5521, Dec. 2016.

[20] W. Yang and J. Zhou, "Wideband low-profile substrate integrated waveguide cavity-backed E-shaped patch antenna," *IEEE Antennas Wireless Propag. Lett.*, vol. 12, pp. 143–146, 2013.

[21] Y. Ge, K. P. Esselle, and T. S. Bird, "E-shaped patch antennas for high-speed wireless networks," *IEEE Trans. Antennas Propag.*, vol. 52, no. 12, pp. 3213–3219, Dec. 2004.

[22] K.-F. Lee, S. L. S. Yang, and A. A. Kishk, "Dual- and multiband U-slot patch antennas," *IEEE Antennas Wireless Propag. Lett.*, vol. 7, pp. 645–647, 2008.

[23] T. H. Jang, H. Y. Kim, D. M. Kang, S. H. Kim, and C. S. Park, "60 GHz low-profile, wideband dual-polarized U-slot coupled patch antenna with high isolation," *IEEE Trans. Antennas Propag.*, vol. 67, no. 7, pp. 4453–4462, Jul. 2019.

[24] S.-H. Wi, Y.-S. Lee, and J.-G. Yook, "Wideband microstrip patch antenna with U-shaped parasitic elements," *IEEE Trans. Antennas Propag.*, vol. 55, no. 4, pp. 1196–1199, Apr. 2007.

[25] H. Sun, Y.-X. Guo, and Z. Wang, "60-GHz circularly polarized U-slot patch antenna array on LTCC," *IEEE Trans. Antennas Propag.*, vol. 61, no. 1, pp. 430–435, Jan. 2013.

[26] K. L. Lau and K. M. Luk, "A wideband dual-polarized L-probe stacked patch antenna array," *IEEE Antennas Wireless Propag. Lett.*, vol. 6, pp. 529–532, 2007.

[27] Y. X. Guo, C. L. Mak, K. M. Luk, and K. F. Lee, "Analysis and design of L-probe proximity fed-patch antennas," *IEEE Trans. Antennas Propag.*, vol. 49, no. 2, pp. 145–149, Feb. 2001.

[28] J. Park, H.-G. Na, and S.-H. Baik, "Design of a modified L-probe fed microstrip patch antenna," *IEEE Antennas Wireless Propag. Lett.*, vol. 3, pp. 117–119, 2004.

[29] K. D. Xu, H. Xu, Y. Liu, J. Li, and Q. H. Liu, "Microstrip patch antennas with multiple parasitic patches and shorting vias for bandwidth enhancement," *IEEE Access*, vol. 6, pp. 11624–11633, 2018.

[30] J. Lin and Q. Chu, "Enhancing bandwidth of CP microstrip antenna by using parasitic patches in annular sector shapes to control electric field components," *IEEE Antennas Wireless Propag. Lett.*, vol. 17, no. 5, pp. 924–927, May 2018.

[31] G.-Y. Chen and J.-S. Sun, "A printed dipole antenna with microstrip tapered balun," *Microw. Opt. Technol. Lett.*, vol. 40, no. 4, pp. 344–346, Feb. 2004.

[32] W. R. Deal, N. Kaneda, J. Sor, Y. Qian, and T. Itoh, "A new quasi-Yagi antenna for planar active antenna arrays," *IEEE Trans. Microw. Theory Techn.*, vol. 48, no. 6, pp. 910–918, Jun. 2000.

[33] P. R. Grajek, B. Schoenlinner, and G. M. Rebeiz, "A 24-GHz high-gain Yagi–Uda antenna array," *IEEE Trans. Antennas Propag.*, vol. 52, no. 5, pp. 1257–1261, May 2004.

[34] R. A. Alhalabi and G. M. Rebeiz, "High-efficiency angled-dipole antennas for millimeter-wave phased array applications," *IEEE Trans. Antennas Propag.*, vol. 56, no. 10, pp. 3136–3142, Oct. 2008.

[35] S. X. Ta, H. Choo, and I. Park, "Broadband printed-dipole antenna and its arrays for 5G applications," *IEEE Antennas Wireless Propag. Lett.*, vol. 16, pp. 2183–2186, 2017, doi: 10.1109/LAWP.2017.2703850.

[36] G. Yang, J. Li, J. Yang, and S. -G. Zhou, "A wide beamwidth and wideband magnetoelectric dipole antenna," *IEEE Trans. Antennas Propag.*, vol. 66, no. 12, pp. 6724–6733, Dec. 2018.

[37] Z. Zhang, Y. Zhao, D. Wu, S. Zuo, L. Ji, X. Yang, and G. Fu, "Dual-polarised crossed-dipole antenna with improved beamwidth," *IET Microw., Antennas Propag.*, vol. 12, no. 6, pp. 890–894, May 2018.

[38] H. Wang, K. E. Kedze, and I. Park, "A high-gain and wideband series-fed angled printed dipole array antenna," *IEEE Trans. Antennas Propag.*, vol. 68, no. 7, pp. 5708–5713, Jul. 2020.

[39] M. A. Amer, M. M. Abdalla, and A. A. Abograin, "Wideband angled dipole array antenna with a suppressed sidelobe levels for beamforming applications," in *Proc. IEEE 2nd Int. Maghreb Meeting Conf. Sci. Techn. Autom. Control Comput. Eng. (MI-STA)*, May 2022, pp. 485–491.

TAE HWAN JANG (Member, IEEE) received the B.S. degree from the Department of Electronic Engineering, Hanyang University, Seoul, South Korea, in 2014, and the Ph.D. degree in electronic engineering from the Korea Advanced Institute of Science and Technology (KAIST), Daejeon, South Korea, in 2019. From 2020 to 2022, he was a Staff Researcher with the Samsung Advanced Institute of Technology (SAIT), Suwon, South Korea. Since 2022, he has been with Hanyang University ERICA, Ansan, Gyeonggi-do, South Korea, where he is currently an Assistant Professor. His research interests include millimeter-wave antenna, and CMOS RF circuits and systems.

AHNWOO LEE was born in Seoul, South Korea, in 1996. He received the B.S. degree in electronic engineering from Hanyang University ERICA, Ansan, South Korea, in 2021, where he is currently pursuing the M.S. degree in electronic engineering. His current research interests include power amplifier, phase shifter, phased array antenna system using GaAs pHEMT, and CMOS process.

SUNGHYUK KIM was born in Seoul, South Korea, in 1996. He received the B.S. degree in electronic engineering from Hanyang University ERICA, Ansan, South Korea, in 2020, where he is currently pursuing the Ph.D. degree in electronic engineering. His current research interests include high powered antenna switch integrated circuits (IC) and LNA IC for mobile communication.

HEE SUNG LEE received the B.S. degree in electrical and electronic engineering from Yonsei University, Seoul, South Korea, in 2014, and the Ph.D. degree in electronic engineering from the Korea Advanced Institute of Science and Technology (KAIST), Daejeon, South Korea, in 2020. From 2020 to 2022, he was a Senior Engineer with SK Hynix, Incheon, South Korea. Since March 2022, he has been with the 6G Research Team, Samsung Research, Samsung Electronics, Seoul. His research interests include CMOS RF/millimeter-wave/THz transceiver and frequency synthesizer.

JAESUK LEE was born in Seoul, South Korea, in 1980. He received the B.S. degree in communication engineering from Daejin University, Gyeonggi-do, South Korea, in 2007, and the M.S. and Ph.D. degrees from the Department of Electronic, Computer and Communication Engineering, Hanyang University, Seoul, South Korea, in 2014.

From 2014 to 2016, he was a Research Engineer with Samsung Electronics. Since 2016, he has been a Principal Engineer with the Electrical Standards Center, Industrial Standards Division, Korea Testing Laboratory. His research interests include the development of broadband antenna design for mobile handset, near-field communication and calibration methods of devices for measuring RF, electromagnetic field, and antenna.

HOON-GEUN SONG received the B.S. degree in electrical engineering from Hanyang University, Ansan, South Korea, in 1998, and the M.S. and Ph.D. degrees in communications and system from Hanyang University, Seoul, South Korea, in 2000 and 2019, respectively. In 2000, he joined LG Electronics, Anyang, Gyeonggi-do, South Korea, working in the area of the multipath searcher and the time tracker for the WCDMA UE modem development. In 2002, he was with Samsung Electronics, Suwon-si, South Korea, in the mobile communication research complex of the Fourth Generations Mobile Communications. Since 2006, he has been the Chief Engineer. He is currently with the Korea Testing Laboratory, Ansan. His research interests include 5G and beyond-5G mobile communication technologies.

JUNG HYUN KIM (Senior Member, IEEE) was born in Busan, South Korea. He received the Ph.D. degree in electrical engineering from Seoul National University, Seoul, South Korea, in 2005. In 2000, he was a Student Co-Founder with WavICs, a power amplifier design company, which is now fully owned by Broadcom, where he invented the switchless stage-bypass power amplifier architecture called CoolPAM. From 2005 to 2007, he was with the Wireless Semiconductor Division, Avago Technologies, as a Group Manager of the Integrated Circuit Design Group. In 2007, he joined the Division of Electrical Engineering, Hanyang University ERICA, Ansan, South Korea, as a Faculty Member, where he is currently a Professor. From 2007 to 2018, he was the External Director with Broadcom. He holds more than 60 U.S. patents on power-amplifier technology and RF integrated circuits. His current research interests include monolithic microwave integrated circuit design for mobile communication and millimeter-wave systems, the thermal packaging analysis of high power devices, and intermodulation and noise analysis of nonlinear circuits.